Salinity Sensor

Prepared by:
Cameron Clark Department of Electrical Engineering
University of Cape Town

Prepared for:
Justin Pead
Department of Electrical Engineering
University of Cape Town

October 11, 2024

Submitted to the Department of Electrical Engineering at the University of Cape Town in partial fulfilment of the academic requirements for a Bachelor of Science degree in Mechatronics

Keywords: Salinity, Sensor, Conductivity, Temperature, Water, Measurement, Electronics, PCB

Declaration

1. I know that plagiarism is wrong. Plagiarism is to use another's work and pretend that it is one's own.
2. I have used the IEEE convention for citation and referencing. Each contribution to, and quotation in, this report .... from the work(s) of other people has been attributed and has been cited and referenced. Any section taken from an internet source has been referenced to that source.
3. This report .... is my own work and is in my own words (except where I have attributed it to others).
4. I have not paid a third party to complete my work on my behalf. My use of artificial intelligence software has been limited to ..... (specify precisely how you used AI to assist with this assignment, and then give examples of the prompts you used in your first appendix).
5. I have not allowed and will not allow anyone to copy my work with the intention of passing it off as his or her own work.
6. I acknowledge that copying someone else's assignment or essay, or part of it, is wrong, and declare that this is my own work

October 11, 2024

Cameron Clark

Date

Acknowledgements

Abstract

Contents

List of Figures

Abbreviations

‰ Parts Per Thousand

ADC Analogue to Digital Converter

CTD Conductivity, Temperature, Depth

DAC Digital to Analogue Converter

EMI Electromagnetic Interference

ENIG Electroless Nickel Immersion Gold

FPU Floating Point Unit

PCB Printed Circuit Board

ppm parts per million

PSU Practical Salinity Units

SST Sea Surface Temperature

Chapter 1

Introduction

Antarctica is the coldest continent on Earth covered in a vast sheet of ice that contains about 30 million cubic kilometres of ice [3] which is about 60% of the world's fresh water. This ice sheet is currently melting at an increasing rate due to global warming and other factors and scientists are trying to understand why. One of the methods being used to analyse sea ice is drilling ice cores and analysing the ice for various properties from the concentration of gases to the concentration of dust particles. One of the properties that is currently difficult to analyse is the salinity of the melted and solid sea ice. This project aims to develop a system that can measure the salinity of the melted sea ice at the bottom of the ice cores mentioned.

1.1 Background

m̃ore about the project sea ice and what this analysis will help with.

1.2 Objectives

The objectives of this project are to create a device that is able to measure the salinity of sea ice at the bottom of ice cores. The device should be able to measure the salinity of the ice in harsh conditions and cold environments that will be present in Antarctica. The device should also be able to measure the salinity of the ice in a non-destructive manner so that the ice core can be used for other analysis after the salinity has been measured.

1.3 System Requirements

Lorem ipsum dolor sit amet, consectetuer adipiscing elit. Ut purus elit, vestibulum ut, placerat ac, adipiscing vitae, felis. Curabitur dictum gravida mauris. Nam arcu libero, nonummy eget, consectetuer id, vulputate a, magna. Donec vehicula augue eu neque. Pellentesque habitant morbi tristique senectus et netus et malesuada fames ac turpis egestas. Mauris ut leo. Cras viverra metus rhoncus sem. Nulla et lectus vestibulum urna fringilla ultrices. Phasellus eu tellus sit amet tortor gravida placerat. Integer sapien est, iaculis in, pretium quis, viverra ac, nunc. Praesent eget sem vel leo ultrices bibendum. Aenean faucibus. Morbi dolor nulla, malesuada eu, pulvinar at, mollis ac, nulla. Curabitur auctor semper nulla. Donec varius orci eget risus. Duis nibh mi, congue eu, accumsan eleifend, sagittis quis, diam. Duis eget orci sit amet orci dignissim rutrum.

1.4 Scope & Limitations

The scope of this project includes the design and development of a device that can measure the salinity of sea ice at the bottom of ice cores. It includes the calibration of the devices, calculations for it, and establishing the accuracy of the device. The scope does not include the capture and analysis of the data from the device.

It is limited to performing in the conditions of Anartica and measureing melted sea ice. It is limited by a budget of R2000 for the full design and development of the device.

1.5 Report Outline

Lorem ipsum dolor sit amet, consectetuer adipiscing elit. Ut purus elit, vestibulum ut, placerat ac, adipiscing vitae, felis. Curabitur dictum gravida mauris. Nam arcu libero, nonummy eget, consectetuer id, vulputate a, magna. Donec vehicula augue eu neque. Pellentesque habitant morbi tristique senectus et netus et malesuada fames ac turpis egestas. Mauris ut leo. Cras viverra metus rhoncus sem. Nulla et lectus vestibulum urna fringilla ultrices. Phasellus eu tellus sit amet tortor gravida placerat. Integer sapien est, iaculis in, pretium quis, viverra ac, nunc. Praesent eget sem vel leo ultrices bibendum. Aenean faucibus. Morbi dolor nulla, malesuada eu, pulvinar at, mollis ac, nulla. Curabitur auctor semper nulla. Donec varius orci eget risus. Duis nibh mi, congue eu, accumsan eleifend, sagittis quis, diam. Duis eget orci sit amet orci dignissim rutrum.

Chapter 2

Literature Review

2.1 A Brief History of Salinity

The most commonly understood definition of salinity relates it to the total amount of dissolved *salts* in a solution, however, salinity's definition has had several more complex iterations over the years. One of the first definitions of salinity was the total amount of dissolved *material* in grams in one kilogram of water [4]. This is a dimensionless quantity that was expressed in Parts Per Thousand (‰) or $g.kg^{-1}$ where most ocean's salinity fell between 34.60‰ and 34.80‰ as shown in Figure 2.1.

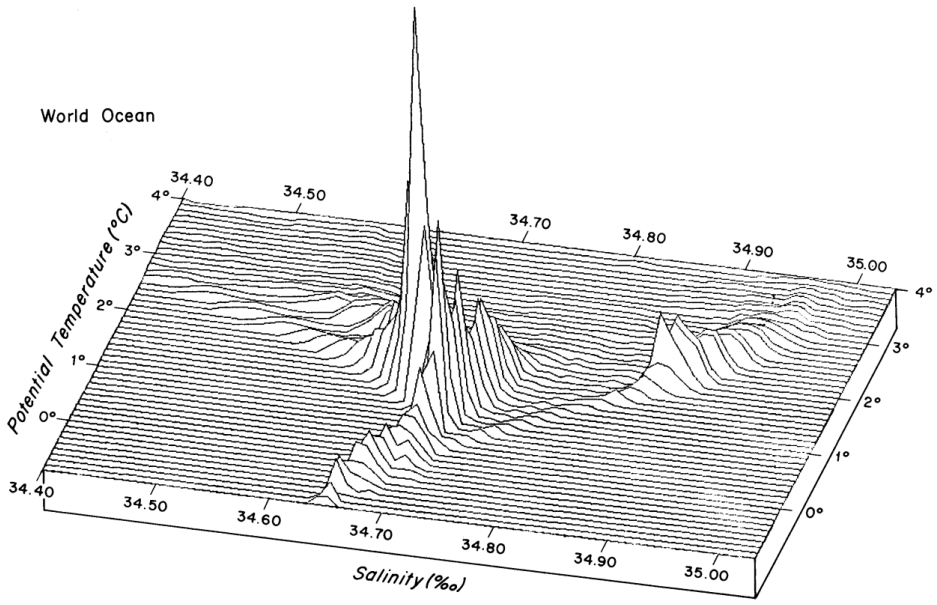

Figure 2.1: Histogram showing the volume of ocean water relative to temperature and salinity bins. The highest peak corresponds to a volume of 26 million cubic kilometres of ocean water [1].

The problem with this definition of salinity lay with its testability. Trying to obtain the mass of the dissolved material through evaporation removed certain compounds making this method inaccurate [5] and other methods of isolating the mass of the dissolved material had similar issues. Salinity needed to be redefined in a way that was easily and reliably testable which led to the next definition of salinity which related salinity related it to the amount of chlorine present in the water, or the chlorinity of the water and in 1969, salinity was redefined to be directly proportional to the chlorinity of the water [4]. The calculation of salinity from chlorinity is further discussed in Section 2.2.1.

Around the same time as the salinity-chlorinity relationship was established, oceanographers had begun experimenting with using conductivity to measure salinity. Conductivity was found to be more precise and significantly easier to measure than the titration required to measure chlorinity [6]. In 1978, the Practical Salinity Scale was established and salinity was redefined to be related to conductivity which is the current definition of salinity[6]. This relationship also included terms for temperature and depth as these affect the conductivity of an electrolyte solution [7].

The Practical Salinity Scale uses its own dimensionless units of salinity which are not interchangeable with ‰ in the current definition of salinity. Although the Practical Salinity Scale is sometimes given in Practical Salinity Units (PSU), it is more technically correct to refer to it as a certain Practical Salinity 'on the Practical Salinity Scale PSS-78' [6]. The calculation of salinity from conductivity is further discussed in Section 3.1.

2.2 Salinity Measurement Methods

Salinity has had a long history of being measured using a variety of methods with varying degrees of accuracy. Currently, the most common method of measuring salinity is through the use of a Conductivity, Temperature, Depth (CTD) instrument, but there are several other methods to achieve this, most of which have been developed over the last 3 decades.

2.2.1 Salinity from Chlorinity

The chemical composition of ocean water with a salinity of 35‰ contains 19.35‰ of Chlorine and 10.77‰ of Sodium with the next most common ions only accounting for just above 3‰ of the total dissolved solids in the water [8]. This allowed oceanographers to estimate that the salinity of ocean water was directly proportional to the amount of chlorine in the water. The chlorinity of a solution had an established definition which was 'the mass of silver required to precipitate completely the halogens in 0.328 523 $4kg$ of the ocean-water sample' [9] which could be tested using titration. In 1969, an accurate relationship between these was established by Reference [9] and thus salinity S was redefined using chlorinity Cl as shown in Equation 2.1.

$$S(‰) = 1.80655 \times \ Cl(‰) \tag{2.1}$$

accuracy achieved?, device?, limitations?

2.2.2 Salinity from Conductivity

The conductivity of a liquid is a measure of the ability of the water to conduct an electrical current which is related to the number of free electrons present in the liquid which is in turn related to the number of ions present in the liquid. In the case of salt water, the ions present are from the dissolved material which is what salinity was previously defined on. The relationship between salinity and conductivity takes into account all the ions present in the water and thus was a more apt measure of salinity than chlorinity which is why salinity was redefined in terms of salinity. Calculating salinity from conductivity requires several equations as it needs correction for both temperature and pressure. These equations are further discussed in Section 3.1. *accuracy achieved?, device?, limitations?*

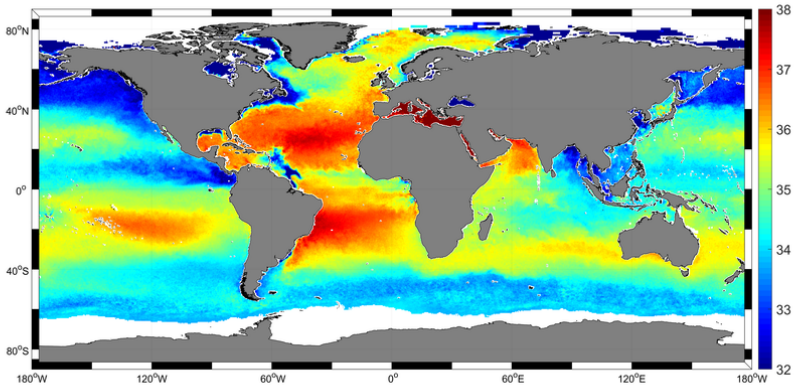

Figure 2.2: Global salinity map generated using satellite data [2].

2.2.3 Salinity from Density

The density of pure water varies with temperature and is considered to be approximately $1000kg.m^{-3}$ at $4°C$ [10]. Adding denser materials to the water will intuitively increase its density and this change can be measured to determine the quantity of dissolved material in the water which relates to salinity. The relationship between salinity and density could be approximated to be linear as shown in Equation 2.2 where ρ is the density of the water, ρ_0 is the density of pure water, k is a proportionality constant, and S is the salinity of the water [11][12].

$$\rho = \rho_0(1 + kS) \tag{2.2}$$

This relationship was further refined to included temperature into the relationship [13]. Reference [13] claimed that density was a better measure of salinity than conductivity as the standard potassium chloride solution used to calibrate the CTDs meters did not account for non-conductive material commonly present in salt water while the density of the water did, however salinity remained defined in terms of conductivity. *accuracy achieved?, device?, limitations?*

2.2.4 Salinity from Microwave Radiation

The electromagnetic spectrum interacts with salt water in unique ways, scattering, refracting and reflecting when in comes in contact with the water and any material dissolved in the water. Different temperature molecules in the water scatter electromagnetic waves differently and the pressure of the water can also affect this, but the most significant effect on the microwave radiation is from the presence of dissolved material in the water [14].

Microwave radiation is one section of the electromagnetic spectrum that take advantage of this fact to measure salinity [14]. The relationship between salinity and microwave radiation is complex but since microwave radiation does not require direct contact with the water, it is possible to measure the salinity of a sample of water from a far distance including from space [15]

This has allowed for the development of satellites that can measure the salinity which have been used to develop global salinity maps as shown in Figure 2.2. The data measured using this method is reported to be accurate to within 0.1 on the Practical Salinity Scale PSS-78 [16], but this method requires multiple different readings to be taken in order to account for the different factors that affect

the microwave radiation including Sea Surface Temperature (SST), surface air pressure, surface air temperature, faraday rotation, and surface wind speed [16].

2.2.5 Salinity from Refractive Index

The second measurement method that takes advantage of the electromagnetic spectrum interaction with salt water uses the visible light spectrum to measure the refractive index of the water. The relationship between salinity and refractive index is complex requiring a 27 term equation which includes the effect of pressure and temperature on the water's refractive index. The refractive index equation is defined a range of $500 - 700nm$ in wave length, $0 - 30°C$ in temperature, and $0 - 40$ on the Practical Salinity Scale PSS-78, and $0 - 11000dbar$ in pressure. The equation holds an accuracy of $0.4 - 80$ parts per million (ppm) on the Practical Salinity Scale PSS-78, decreasing with increasing pressure. [17]

A refractometer is the device that is used to measure the refractive index of the water, and due to only needing a small amount of the sample, these devices can be quite compact. A few researches have developed compact refractometers, the notable ones of which have dimensions of $22.5mm \times 22.5mm \times 120mm$ [18] and $40mm \times 40mm \times 70mm$ [19] which achieved accuracies of 2 and 83 ‰ on the Practical Salinity Scale PSS-78 respectively.

2.2.6 Salinity from Interferometry

The last measurement methods that takes advantage or the electromagnetic spectrum interaction with salt water is interferometry. Interferometry involves generating two identical light waves one the visible spectrum and then passing one through the sample and then comparing the two waves to identify the phase shift and gain. These measurements can be used to identify the salinity of a sample of salt water [20].

This method has varying implementation with varying results with Reference [21] reporting accuracies down to 0.001 on the Practical Salinity Scale PSS-78 using a Michelson interferometer which other researches have reported other accuracies using different methods [22][23][24]. The refractometer does have the disadvantage of being large instrument as the mirrors required to direct the light waves require space and precise alignment making this a difficult method to implement in a compact device.

2.2.7 Salinity from Electromagnetic Induction

Similarly to conductivity, the magnetic permeability of a liquid is related to the number of ions present in the liquid. The more ions present in the liquid, the stronger the magnetic field that can be generated by the liquid which increases the magnetic permeability of the liquid which is related to the total dissolved solids in salt water's case [25].

There are several methods of measuring the magnetic permeability of a liquid that all involve inducing a magnetic field in the liquid and then measuring its response. These methods all have the advantage of not requiring direct contact with the salt water to make the measurement which allows for the sample to remain undisturbed unlike the conductivity method [26]. This method has not been fully investigated however the equipment that is required to measure the magnetic permeability of a liquid

is relatively large and requires a lot of power to operate which makes it difficult to implement in a compact device for use in remote environments.

2.3 Salinity Measurement Devices using Conductivity

Chapter 3

Theory Development

3.1 The Calculation of Salinity From Conductivity

Salinity meters that use electrical conductivity are commonly known as CTDs. As depth is a measurement derived from pressure, CTp is the preferred designation when performing calculations [6]. This allows for the conductivity of a sample of water to be denoted by $C(S, T, p)$ where conductivity is a function of salinity S, temperature T, and pressure p which is the convention in oceanography [6]. Pressure in the salinity equation is taken relative to sea level where $p = 0dbar$ is equivalent to an absolute pressure of $P = 101\ 325Pa$ [27]. Using decibars (dbar) for pressure is a common practice in oceanography as it is a unit of pressure that is equal to roughly one meter of water depth [28].

The Practical Salinity Scale defines Practical salinity S_p in terms of a conductivity ratio K_{15} which is the conductivity of a sample of water at a temperature of $15°C$ and a pressure equal to one standard atmosphere divided by the conductivity of a standard potassium chloride solution at the same temperature and pressure. The standard potassium chloride solution is $32.4356g$ of KCl dissolved in $1.000kg$ of water and when the ratio between the conductivity of a sample of water and the standard solution, or K_{15}, equals 1 the Practical Salinity S_p is, by definition, 35. [27]

When K_{15} is not equal to 1, the Practical Salinity S_p can be calculated using the PSS-78 equation shown in Equation 3.1.

$$S_p = \sum_{i=0}^{5} a_i (K_{15})^{i/2} \quad \text{where} \quad K_{15} = \frac{C(S_p, 15°C, 0)}{C(35, 15°C, 0)} \tag{3.1}$$

All the coefficients for the salinity-conductivity equations, including a_i, are given in Table 3.1.

To calculate the salinity of a sample of water that is not at $15°C$ and $0dbar$, the conductivity ratio of the sample can be expanded into the product of three ratios which are labelled R_p, R_t, and r_t respectively. The conductivity measurement taken in the field $C(S_p, t, p)$ is related to the conductivity of the standard solution $C(35, 15°C, 0)$ which the device is calibrated with and is represented by R in Equation 3.2. [27]

$$R = \frac{C(S_p, t, p)}{C(35, 15°C, 0)} = \frac{C(S_p, t, p)}{C(S_p, t, 0)} \cdot \frac{C(S_p, t, 0)}{C(35, t, 0)} \cdot \frac{C(35, t, 0)}{C(35, 15°C, 0)} = R_p R_t r_t \tag{3.2}$$

check In order to calculate the salinity of the sample R_t must be found which takes a similar for to

K_{15}. r_t is first calculated using the temperature of the sample

$$r_t = \sum_{i=0}^{4} c_i t^i \tag{3.3}$$

following which R_p is calculated using the sample's pressure p, temperature t and conductivity ratio R,

$$R_p = 1 + \frac{\sum_{i=1}^{3} e_i p^i}{1 + d_1 t + d_2 t^2 + R\,[d_3 + d_4 t]} \tag{3.4}$$

and finally R_t is calculated using r_t, R_p and R.

$$R_t = \frac{R}{R_p r_t} \tag{3.5}$$

Note that for a sample temperature of $15°C$ and pressure of $0dbar$, r_t and R_t both equal 1 which leaves R_t equal to R and thus Equation 3.1 can be used to calculate the Practical Salinity S_p. For temperatures other than $15°C$, the Practical Salinity S_p can be calculated using Equation 3.6 where $k = 0.0162$. [27]

$$S_p = \sum_{i=0}^{5} a_i (R_t)^{i/2} + \frac{t - 15}{1 + k(t - 15)} \sum_{i=0}^{5} b_i (R_t)^{i/2} \tag{3.6}$$

Table 3.1: Coefficients for the PSS-78 equations [27].

i	a_i	b_i	c_i	d_i	e_i
0	0.0080	0.0005	$6.766097 \cdot 10^{-1}$		
1	−0.1692	−0.0056	$2.00564 \cdot 10^{-2}$	$3.426 \cdot 10^{-2}$	$2.070 \cdot 10^{-5}$
2	25.3851	−0.0066	$1.104259 \cdot 10^{-4}$	$4.464 \cdot 10^{-4}$	$-6.370 \cdot 10^{-10}$
3	14.0941	−0.0375	$-6.9698 \cdot 10^{-7}$	$-4.215 \cdot 10^{-3}$	$3.989 \cdot 10^{-15}$
4	−7.0261	0.0636	$1.0031 \cdot 10^{-9}$	$-3.107 \cdot 10^{-3}$	
5	2.7081	−0.0144			

Note that the coefficients a_i precisely sum to 35 such that the Practical Salinity S_p is 35 when K_{15} or $R_t = 1$ as per Equation 3.1 and Equation 3.6. Additionally, the coefficients b_i precisely sum to 0 such that the Practical Salinity S_p does not depend on the temperature of the water when $R_t = 1$ as per Equation 3.6. [27]

Equation 3.1 to Equation 3.6 are valid for $2 < S_p < 42$ and $-2°C < t < 35°C$ and $0dbar < p < 10\ 000dbar$ [27]. The range for salinity has been extended using estimations by Reference [29] for $0 < S_p < 2$ and Reference [30] for $42 < S_p < 50$.

The temperatures used in Equation 3.1 to Equation 3.6 are on the IPTS-68 scale [31] and have not been corrected to the currently used ITS-90 scale [32]. In order to correctly calculate the salinity, the temperatures should be converted to the IPTS-68 scale using the equation $t_{68} = 1.00024 t_{90}$ before

calculating salinity [32].

3.2 Electrical Characteristics of Salt Water

PSU vs TSD vs conductivity vs resistivity, salinity equation, capacitance of salt water, non-constant conductivity vs voltage.

3.3 Electrical Fringing in Conductive Materials

Chapter 4

Design

4.1 Salinity Measurement Method

The most common method of measuring salinity is to measure the conductivity of the water and then calculate the salinity using the conductivity and temperature of the water. This is most commonly done using a CTD which takes all three measurements simultaneously. Measuring conductivity, temperature and depths was the most desirable method for this project as it was the industry standard, the author had significant experience with Printed Circuit Board (PCB) design and electronics, and it was the most likely device to be able to fit in the ice core. While the other methods of measuring salinity have provided interesting results, refractometers and chlorinity titrations were not fully automatable, microwave radiation and densitometers were expensive and complex, and electromagnetic induction and interferometry required complex, calibrated equipment.

4.2 Conductivity Electrode Material

Ideal electrodes for measuring conductivity in salt water need to have zero resistance, infinite corrosion resistance and be able to confine the electrical current in the water to a specific known volume. Electrodes with zero resistance would allow the resistance measured using the electrodes to be entirely due to the water; although most conductive materials have a conductivity in the order of $10^8 Sm^{-1}$ which causes negligible resistance compared salt water which has a conductivity range of $0-5 Sm^{-1}$ [33]. The infinite corrosion resistance will allow the electrodes to last indefinitely in the highly corrosive salt water environment and there are several materials with near perfect corrosion resistance that are used in marine environments. The confinement of the electrical current allows for an easier calculation of the conductivity ρ from resistance R if the cross-sectional area A and length l of the water between the electrodes is known as shown by Equation 4.1.

$$\rho = \frac{RA}{l} \tag{4.1}$$

The several materials that are known for their corrosion resistance include the non-precious metals aluminium, stainless steel, nickel and copper alloys, and titanium as well as the precious metals gold, silver and platinum. The precious metals are known for having a significantly higher corrosion resistance however they are also significantly more expensive.

The choice of material aimed at using materials with the highest corrosion resistance while still choosing materials that were attainable and within this project's budget. Titanium is the most corrosive resistant

of the non-precious metals and has an acceptable conductivity of $2.3 \cdot 10^6$ which is about 25 less than that of copper [34]. Titanium wire was available through off-cuts from a project being conducted by the Chemical Engineering Department of the University of Cape Town, and thus it was possible to use this material for the electrodes.

Of the precious metals, gold is one of the most accessible as it is a common material used in PCBs manufacturing primarily because of its high corrosion resistance while it maintains a high conductivity of $49 \cdot 10^6$ which is similar to copper [34]. Electroless Nickel Immersion Gold (ENIG) PCB manufacturing is a process where nickel followed by gold are deposited onto the copper of the PCB using chemical reactions. While this process is expensive compared to standard PCB manufacturing, it is affordable within this project's budget and made gold a possible material for the electrodes.

Both gold and titanium were used for this project as the two electrodes were able to manufactured into two different shapes which allows for comparative testing of the two materials.

4.3 Conductivity Electrode Design

Gold electrodes made using the ENIG PCB manufacturing process were chosen to be the primary electrodes for the device. The PCB manufacturing process allowed the electrodes to be made with a known area and length of the water between the electrodes which would allow for a more accurate calculation of the conductivity.

Some scientific papers that attempt to measure salinity have an uncertainty on whether salt water has a constant resistivity relative to the voltage applied to it or not. In order to verify this, the resistance of the water between the electrodes needed to be measured at different voltages while other factors were kept constant which necessitated close attention to the fringing effect of the electrical current between the electrodes. Thus, wide, flat pads were used on the PCB electrodes which were placed close together to reduce the amount of current fringing. Additionally, a fringe guard was added to the electrodes which consisted of a pad that outlined the main conductivity pads that repeated the same voltage as the main pads using an op-amp with unity gain. Ideally, the fringe guard would saturate the volume around the main pads with current and thus prevent the main pads from fringing. This design is shown in Figure 4.1.

The dimensions of the gold electrodes were chosen somewhat arbitrarily with the pads having a large area while being placed relatively close together to reduce the fringing but not too close to prevent water from flowing between the pads. Additionally, the aim was to keep the resistance between the pads low to lower the amount of voltage required to generate a current through the water thus further reducing the fringing. The gold electrodes were designed with a $20mm \times 20mm$ pad area with a $2mm$ wide fringe guard surrounding the majority of the pad and the electrodes were spaced $10mm$ apart. This gave a resistance from 3.75Ω to 6.25Ω between the gold electrodes for salinities from 40 to 25 on the Practical Salinity Scale PSS-78 respectively.

The titanium electrodes are substantially simpler and cheaper than the gold electrodes and would be the preferred electrodes if the fringing effect could be mathematically accounted and corrected for. Provided the testing with the gold electrodes is able to prove a constant resistance-voltage relationship,

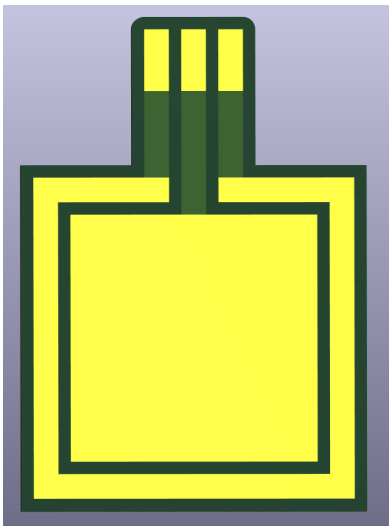

Figure 4.1: The gold electrode PCB design.

the fringing effect between the titanium electrodes could be measured and accounted for allowing for them to be used as the primary electrodes in a future iteration of the device. The titanium wire that was available for this project was $1mm$ in diameter and in order to account for the unknown resistance between the electrodes, the design allowed for an adjustable spacing between the electrodes and adjustable electrode length.

4.4 Resistance Measurement Method

The most common and practical method of measuring resistance is to use a resistor divider circuit which is what this project chose to use. The electrodes were chosen to be the R_2 resistor in the voltage divider and the R_1 resistor was chosen to be a significantly larger, known resistance. This configuration had two advantages: it would reduce the voltage required to generate a current through the water and thus reduce the fringing effect, and it would prevent the board from being short-circuited if the electrodes were to touch as the R_1 resistor would limit the current. The measurement taken from the voltage divider was then amplified using an op-amp to increase the resolution of the voltage measurement.

4.5 Circuit Overview

Figure 4.2 shows a simplified overview of the resistance measuring circuit that was used in this project. The circuit was designed to be printed onto a PCB (herewith referred to as the probe) manufactured with `JLCPCB` due to their low cost, ease of manufacturing, precision relative to hand soldering and the familiarity of the author with the process.

The voltage driving the resistor divider was provided by a Digital to Analogue Converter (DAC) such that the voltage could be varied and the resistance-voltage relationship could be determined of the salt water between the electrodes. The DAC model was chosen from the available DACs on the `JLCPCB` website and the DAC53401 was chosen for its high updated rate of $10us$, and it had advanced functionality allowing it to output square, triangle and sawtooth waves which would allow for high

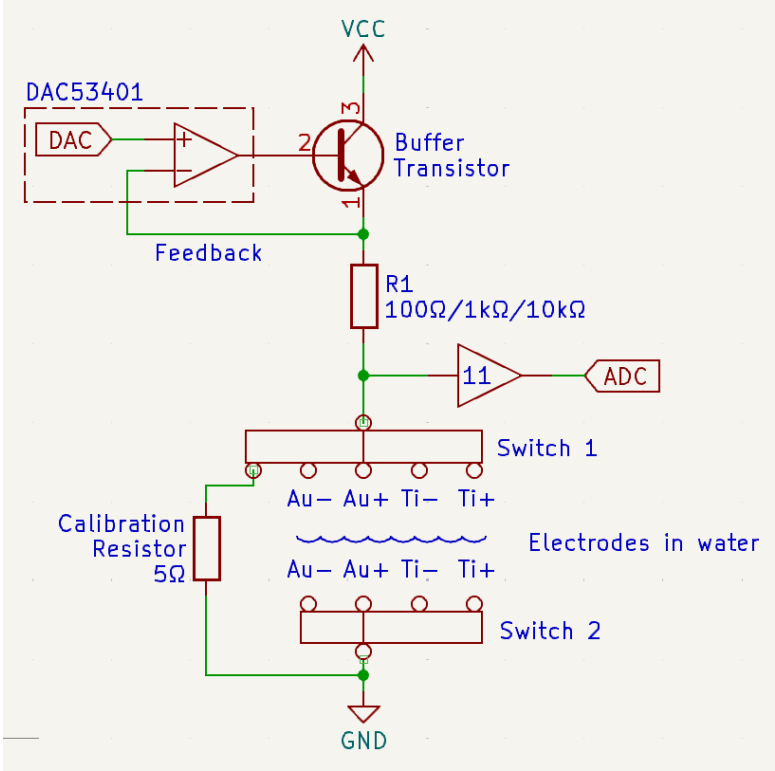

Figure 4.2: A simplified representation of the resistance measuring circuit.

frequency tests. The output DAC was then connected to a buffer transistor and the output of the buffer was connected to the feedback of the DAC. This would allow a higher current to be drawn than what the DAC was rated for while still maintaining the desired output voltage.

The R_1 value that was chosen to pair with the gold electrodes was 100Ω as it was the smallest e12 series resistance that would prevent the board from drawing too much current. Due to the unknown resistance between the titanium electrodes, additional R_1 resistors were added to the board to allow for a range of resistance measurements. Thus, the R_1 values were chosen to be 100Ω, $1k\Omega$ and $10k\Omega$ which would be used when the resistance between the probes is $1\Omega - 10\Omega$, $10\Omega - 100\Omega$ and $100\Omega - 1k\Omega$ respectively. This would allow for a minimum resolution of 11% of V_{CC} for the voltage measurement by the Analogue to Digital Converter (ADC) as shown by Equation 4.2.

$$\frac{1\Omega}{1\Omega + 100\Omega} * 11 = 11\% \tag{4.2}$$

$$\frac{10\Omega}{10\Omega + 100\Omega} * 11 = 100\% \tag{4.3}$$

Switch 1 allows R_1 to be connected to any of the four electrodes or the calibration resistor of 5Ω and switch 2 allows for the other electrode to be connected to ground. For example, switch 1 could be connected to Ti+ and switch 2 could be connected to Ti- to measure the resistance between the titanium electrodes. This configuration also allows current to flow in both directions between electrodes which can prevent an excessive build up of chlorine gas or sodium electroplating on the electrodes by taking a resistance measurement in both directions in rapid succession.

In order to increase the measurement accuracy of the resistance, multiple high accuracy resistors were

placed in series to attain the values of R_1 and the calibration resistor as this decreases the uncertainty of their resistance. This total uncertainty of the parallel resistors $\delta_{R_{total}}$ is decreased by a factor equal to number of parallel resistors n compared to each individual resistor's uncertainty δ_R as shown by Equation 4.4 to Equation 4.6.

$$R_{total} = \left[\sum_{i=1}^{n} \frac{1}{R}\right]^{-1} = \left(\frac{n}{R}\right)^{-1} = \frac{1}{n} \cdot R \tag{4.4}$$

$$\text{for a function } f(x_1, x_2, \ldots, x_n), \text{ its tolerance } \delta_f = \sqrt{\sum_{i=1}^{n} \left(\frac{\partial f}{\partial x_i} \delta x_i\right)^2} \tag{4.5}$$

$$\therefore \delta_{R_{total}} = \sqrt{\left(\frac{\partial R_{total}}{\partial R} \delta_R\right)^2} = \sqrt{\left(\frac{1}{n} \delta_R\right)^2} = \frac{1}{n} \delta_R \tag{4.6}$$

The resistances for R_1 were made from 3 parallel resistors with tolerance $\pm 1\%$ giving a total tolerance of $\pm 0.\bar{3}\%$ and the calibration resistor was made from 4 parallel resistors with tolerance $\pm 1\%$ giving a total tolerance of $\pm 0.25\%$.

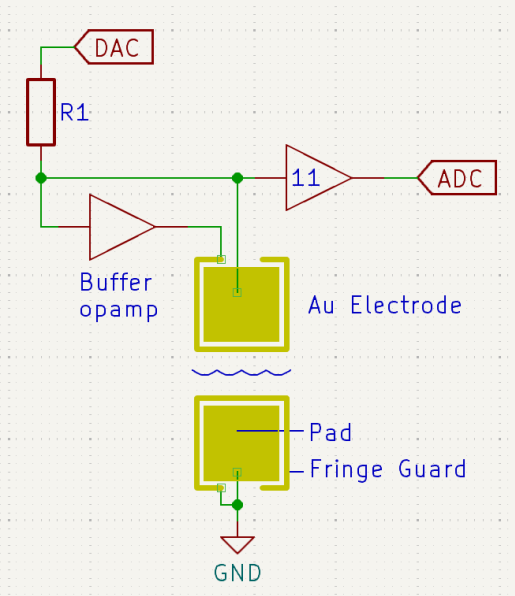

Figure 4.3: A simplified representation of the resistance measurement circuit using the gold electrodes with the fringe guard.

Figure 4.3 shows an example switch configuration where the gold electrodes are used. The voltage from the DAC is routed through the R_1 resistor and then through the gold electrodes pads as well as to a buffer op-amp which repeats the voltage through fringe guard without affecting the voltage between the main pads. A set of switches was also added to electrically disconnect the fringe guards to test for their effectiveness. The fringe guards had the same voltage as the main pads with a lower conductivity so the current flowing between the fringe guards was assumed to be less than that of the pads and thus there was no need to limit the current from the op-amp.

4.6 Salinity Calculation and Display

In order to measure the salinity of the sea ice, the probe PCB needed to be lowered into the water and measure salinity at various depths. There are two methods for capturing the salinity data: either to constantly record the salinity data as the device it lowered through the water column or to have the device take a measurement when instructed by a controller. The former method creates logistical problems with waterproofing the device and retrieving data while the latter was a more user-friendly approach allowing researchers to control exactly which depths the salinity is measured at and thus it was chosen for this project.

The controller was a basic PCB with input buttons, input rotary switches, two 7-segment displays, an RS485 communication port and a simple microcontroller. The RS485 communication port was chosen as the communication protocol as RS485 has the longest range and a high noise resistance which is necessary for the device to be used in the ocean which has high Electromagnetic Interference (EMI). The author was also familiar with the protocol and had previous board to board communication experience with it. The microcontroller was arbitrarily chosen from the STM32F030 series as it was relatively cheap, it did not need to perform any complex calculations, and the author was familiar with the STM microcontroller series.

With an external controller, a waterproofed probe could be lowered into the water and measure the water's salinity. The chosen method of waterproofing probe was to coat it with a layer of epoxy resin to waterproof it as this was the most familiar and cost-efficient method available. In addition to the ports for the conductivity electrodes and the circuitry shown in Figure 4.2, the probe had temperature and depth sensors which are discussed in Section 4.7, an RS485 communication port and a microcontroller. The microcontroller was chosen from the STM32F4 series as STM microcontrollers as they have a Floating Point Unit (FPU) which allowed for the salinity calculation to be performed on the probe.

4.7 Temperature and Depth Measurement

Depth sensors that are waterproof are too expensive for this project's budget. However, there have been alternative approaches which use non-waterproof sensors that are isolated form the water using a flexible membrane that would allow the pressure to be transmitted to the sensor. *[citation needed]* The depth sensor for this project was chosen as the cheapest depth that could handle above 50 meters of water pressure available at `JLCPCB` which was the WF183DE. This project included a depth sensor with the aim to use this method to measure the depth of the probe in the water, however it also included a method for the user to manually input the depth of the probe in the water using the controller should this method fail.

The temperature sensor used in this project was an arbitrarily chosen, surface mount temperature sensor that had high accuracy and a wide temperature range. The temperature sensor should be coated with a thin layer of epoxy resin to waterproof it as epoxy resin is a poor thermal conductor and thus a thinner layer would allow for a more accurate temperature measurement. The choice of microcontroller and pressure sensor also provided this board with two alternative temperature sensors with less accurate, however they could be used in the event that the primary temperature sensor failed.

4.8 PCB Assembly and Corrections

TODO: pcb correction and labelled diagram.

4.9 Probe Code

The major steps in measuring salinity are to measure the conductivity of the water between the electrodes, measure the temperature and pressure of the water and then calculate the salinity. An overview of this process along with steps for each major measurement is shown in Figure 4.4.

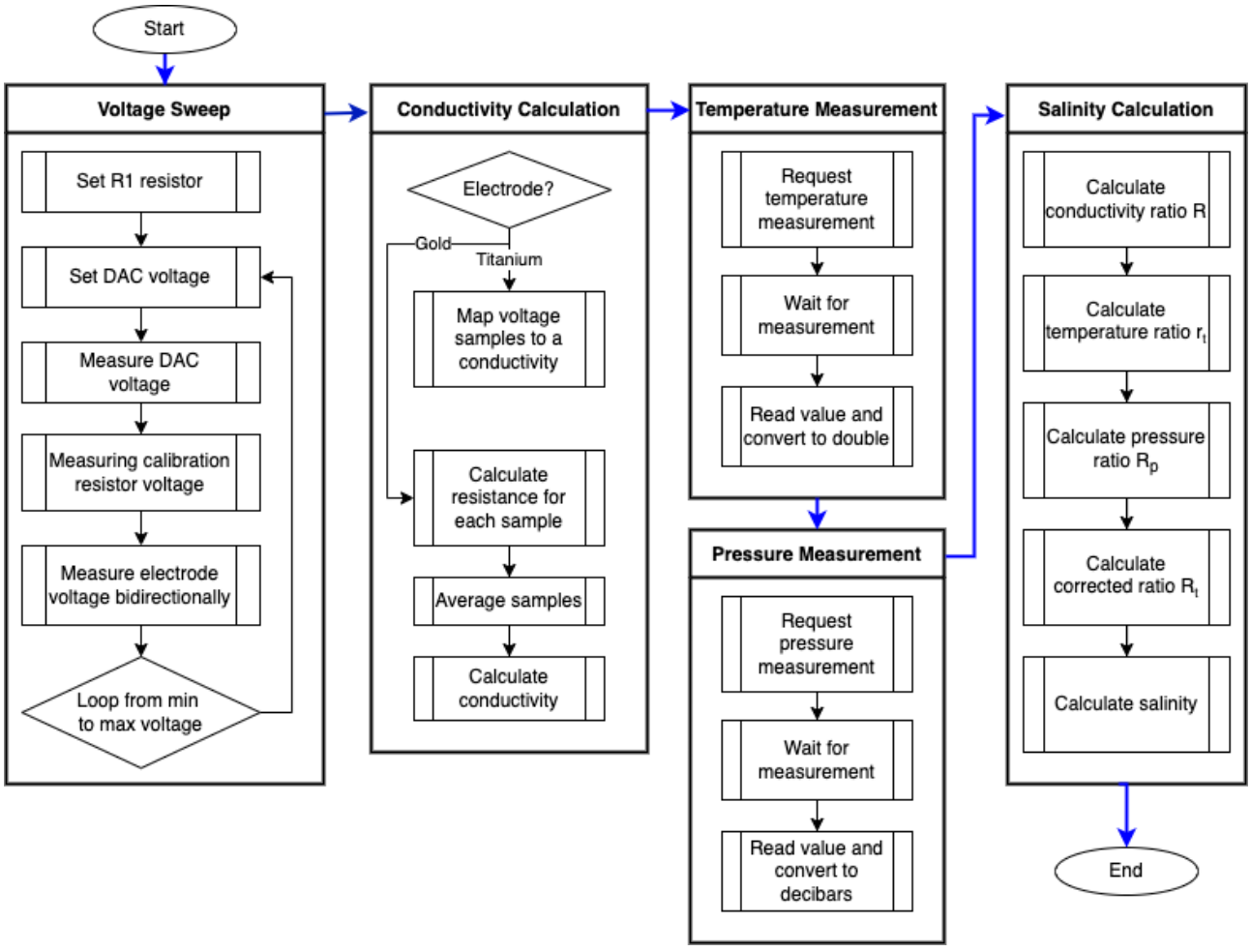

Figure 4.4: The flowchart for the probe code that measures salinity.

The conductivity measurement and calculation is different depending on if the voltage-resistance relationship is constant or not which is expected for the gold and titanium electrodes respectively. Both variations start with a voltage sweep where the voltage is increased from the minimum to the maximum voltage with a set voltage step or vice versa by the DAC. At each step, the voltage output of the DAC, the voltage across the calibration resistor and the voltage across the electrodes are measured.

If the ratio between the DAC voltage and the voltage across the electrodes is not constant, the conductivity will have to be analysed by performing tests to create a model to relate each voltage sample to the conductivity of the water.

If the ratio between the DAC voltage and the voltage across the electrodes is constant, the resistance between the electrodes can be calculated using the calibration resistor. Given that the calibration resistance and R_1 is known, the resistance between the electrodes can be calculated for each voltage sample using the ratio between the electrode and calibration voltages as shown in Equation 4.7. k is calculated using the known values V_{ratio}, R_1 and $R_{calibration}$ to simplify the equation as shown in Equation 4.8 and finally $R_{electrode}$ can be calculated using Equation 4.9.

$$V_{ratio} = \frac{V_{DAC} A_{11} A_{ADC} \frac{R_{electrode}}{R_1 + R_{electrode}}}{V_{DAC} A_{11} A_{ADC} \frac{R_{calibration}}{R_1 + R_{calibration}}} = \frac{\frac{R_{electrode}}{R_1 + R_{electrode}}}{\frac{R_{calibration}}{R_1 + R_{calibration}}} \tag{4.7}$$

$$\frac{R_{electrode}}{R_1 + R_{electrode}} = V_{ratio} \frac{R_{calibration}}{R_1 + R_{calibration}} = k \tag{4.8}$$

$$R_{electrode} = \frac{kR_1}{1 - k} \tag{4.9}$$

The resistance can then be averaged and the conductivity can be calculated for the gold electrodes using Equation 4.1. Using this method allows for the device to nullify all scalar inaccuracies in the circuit including R_1 uncertainty, DAC and ADC gain errors, and the op-amp gain error as they will all be present in the calibration resistor and the electrodes measurements. This method is however still vulnerable to offset inaccuracies including DAC and ADC offset errors and the internal resistance of the switches and traces.

Measuring the temperature and pressure is a simple matter of reading the temperature sensor and the pressure sensor respectively which finally allows salinity to be calculated which can be performed on the salinometer microcontroller as it possesses an FPU. Additionally, any of the temperature, depth, resistance or conductivity measurements can be calculated individually and transmitted to the controller if requested.

4.10 Controller Code

todo

The controller's primary goal is to request measurements and display the returned values to the user. However, once the probe is cast in epoxy resin it will become unprogrammable and thus the controller must also be able to configure the probe's settings. The parameters that the controller will need to adjust include the R_1 resistance, the electrode type, whether to use the fringe shield or not, the voltage sweep range and steps and the number of ADC samples to average.

Chapter 5

Salinometer Evaluation and Testing

The PCB boards were delivered and tested. Some design errors were found which include using op-amps that were rated for 6V instead of 3V3, missing a connection between VDDA and VCC, and footprints errors with both the temperature sensor and depth sensor. The temperature sensor footprint was unable to be corrected, but the depth sensor could be corrected by flipping the depth sensor.

Once the circuitry was working and coded, the salinometer was tested. The testing was conducted in two phases. One phase before the probe was cast into epoxy resin and the other after the probe was cast into epoxy resin (section numbers?). A summary of these tests is shown in Table 5.1 and each test is discussed in further detail in the following sections.

The equipment used to verify these tests were a bench multimeter model Keysight U3401A which had voltage accuracy to 0.02% and resistance accuracy to 0.1%.

Table 5.1: A summary of the evaluation and testing of the salinometer.

Sec.	Test Description	Result Metric	Ideal Result	Measured Results
5.1	The minimum and maximum voltage output of the DAC between $0V$ and $V_{DD} = 3.3V$	Range	$0 - 3.3V$	$0 - 2.83V$
5.1	The gain and offset of the output voltage of the DAC relative to the instructed voltage	Gain Offset	1.0 $0.0V$	0.9837 $0.0070V$
5.2	The gain and offset of the voltage measured by the ADC relative to the voltage measured by the multimeter	Gain Offset	1.0 $0.0V$	0.9877 $0.0082V$
5.3	The resistance of the calibration resistor R_{CAL}	Resistance	5Ω	5.00Ω
5.4	The gain and offset of the resistance measured by the salinometer relative to the resistance measured by the multimeter	Gain Offset	1 0Ω	1.0000 0.0000Ω

5.1 DAC Voltage Range and Accuracy

The DAC configuration uses a transistor in order to buffer the DAC output which allows for the power draw to be support by the transistor instead of the DAC. This is a common configuration where the DAC is connected to the non-inverting input of an op-amp whose output is connected to the base of an

NPN transistor. The emitter of the transistor is then connected to the inverting input of the op-amp which allows the buffered output to match the input of the DAC.

This configuration does have one disadvantage in that the output voltage of the DAC is limited by the transistor's V_{BE} such that the highest voltage output at the emitter of the transistor is $V_{DD} - V_{BE}$. According to the transistor's data sheet, the buffered output should be limited to $3.3V - 0.6V = 2.7V$ when conducting $0A$ and $3.3V - 0.75V = 2.55V$ when conducting the maximum current of $33mA$ when the load is 100Ω. In order to assess the range and accuracy of the DAC, the DAC was instructed to output voltages from $0V$ to V_{DD} in intervals of 64-bits and the output voltage was measured at the base and emitter of the buffer transistor and under maximum load of 100Ω and no load. V_{DD} and GND were measured to be $3.299V$ and $0V$ respectively.

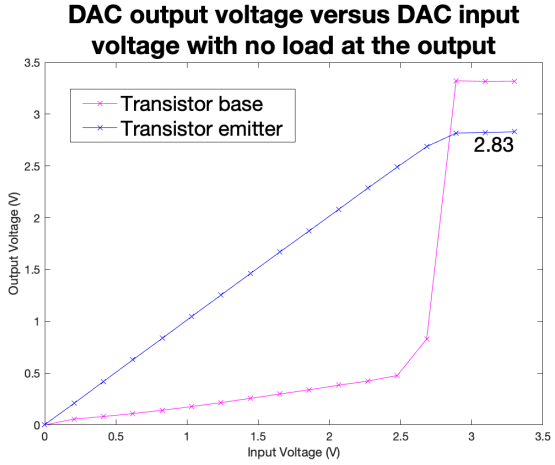

Figure 5.1: The input voltage versus the output voltage of the DAC with no load.

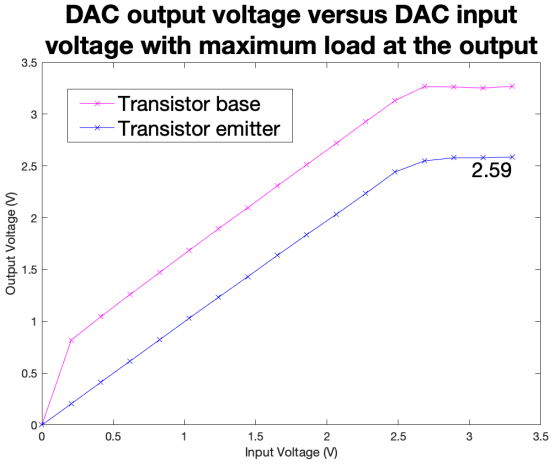

Figure 5.2: The input voltage versus the output voltage of the DAC with a load of 100Ω.

The results were graphed and are shown in Figure 5.1 and Figure 5.2. The voltage drop as a result V_{BE} can clearly be seen on Figure 5.2. The unloaded output voltage was able to reach $2.83V$ and the loaded output voltage was able to reach $2.59V$ which are slightly higher than the predicted limits.

An alternate attempt was also made to achieve a higher voltage output by using the internal reference voltage of the DAC. The internal reference voltage was set to $4 \times 1.21V = 4.84V$ and the DAC was instructed to output the maximum voltage. As expected, this was not able to increase the output voltage; the base of the transistor still outputted $3.3V$ and the emitter still outputted $2.83V$ while unloaded.

Due to the voltage limitations, the DAC will have a limited output in future testing and implementation to prevent the output voltage not reaching the desired input voltage. The output will be limited to $0V$ to $2.5V$ or 0 to 775 for fully loaded tests and the implementation and $0V$ to 2.7 or 0 to 837 for unloaded tests. When excluding the voltage readings above $2.5V$, the DAC was able to achieve a gain of $0.9837V/V$ and an offset $+0.0070V$ between the input voltage and output voltage when under maximum load.

add LSB error = 0.00032V

5.2 ADC Accuracy

The ADC will be tested by measuring a range of voltages produced by the DAC and comparing the voltage measured by a multimeter to the voltage measured by the ADC. The ADC will be configured in 12-bit mode with each measurement taking 15 ADC clock cycles and 5 measurements will be taken and averaged to increase the accuracy of the measurement. The accuracy of the ADC should ideally be 100%.

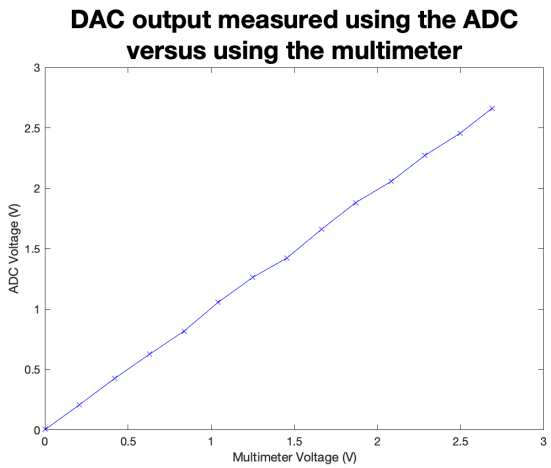

Figure 5.3: The voltage output by the DAC measured by a multimeter versus measured by the ADC.

The results are shown in Figure 5.3. The ADC achieved a gain of $0.9877V/V$ and an offset of $0.0082V$ when compared to the multimeter.

5.3 Calibration Resistance

The calibration resistor will be measured by using the multimeter and by using the ADC with and without the gain applied. The calibration resistance was specified to be $5\Omega \pm 0.25\%$, and thus it is expected to be between 4.9875 and 5.0125Ω.

The calibration resistors were electrically disconnected, and the multimeter was used to measure the calibration resistor to be 5.25Ω when the probes where applied directly across one of the parallel calibration resistor's terminals. The multimeter cables measured 0.25Ω when connected to each other and thus the final resistance of the calibration resistor was 5.00Ω. It should be noted that the multimeter could only measure down to 0.01Ω and thus the true resistance could range from 4.99Ω to 5.01Ω.

5.4 Resistance Measuring Accuracy

The method of measuring resistance involves getting a voltage reading of the calibration resistor and a sample resistor which is attached between the titanium electrode ports. The resistance of the sample resistor is then calculated using the ratio between the voltage across the sample resistor and the calibration resistor.

This will be done using two methods: one with a single voltage from the DAC of $V_{DD}/2 = 1.65V$ and

one with voltage sweep from the DAC with 50 samples. It was noticed during the testing phase that low voltage readings were not accurate as single bit errors caused large changes in the resistance reading and thus the range of voltages will be limited to $0.3V$ to $2.6V$ or 93 to 806 bits. Both measurements will then be compared to the resistance measured by the multimeter. The range of the resistors used will be 0Ω to 10Ω as this is the expected range for the gold electrodes.

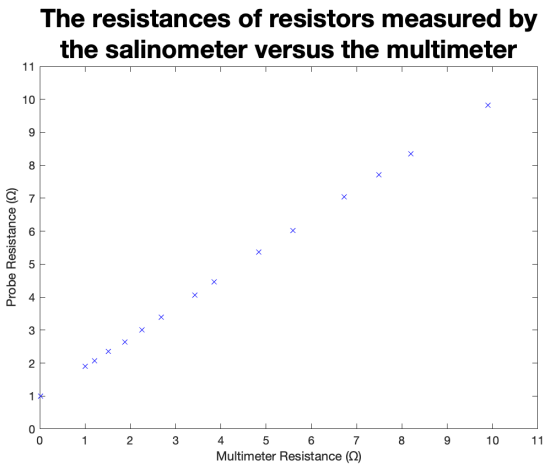

Figure 5.4: The resistance measuring test.

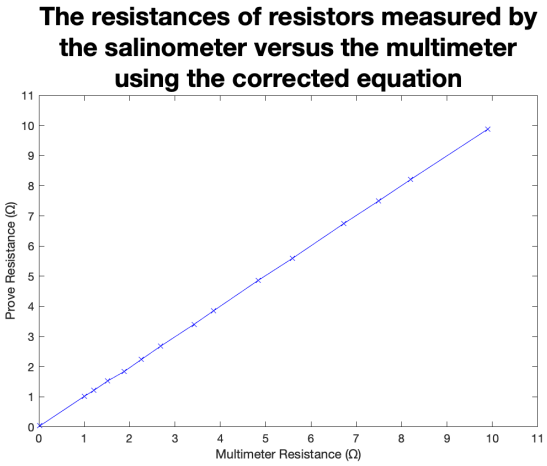

Figure 5.5: The resistance measuring test using the corrected equation.

The results are shown in Figure 5.4. The single voltage method and voltage sweep method were perfectly correlated with an r^2 value of 1.0000, however there was a clear error between the actual resistance and the resistance measured by the salinometer. This error was assumed to be due to the resistance of the switches and the traces. While these values could be measured and corrected for, a more efficient and arguably more accurate method would be to generate a curve of best fit and use this to correct the resistance readings.

In order to generate the equation of best fit, the voltage ratio Equation 4.7 is adjusted to include r_e which represents the resistance of the switches and traces as shown in Equation 5.1. The $R_{calibration}$, R_1 and the r_e the standard rational function coefficients p and q as shown in Equation **??**. Finally, the equation is rearranged to give the resistance of the electrode in terms the measured voltage ratio as shown in Equation 5.2.

$$\begin{aligned} V_{ratio} &= \frac{\frac{R_{electrode} + r_{e1}}{R_{electrode} + R_1 + r_{e2}}}{\frac{R_{calibration} + r_{e3}}{R_{calibration} + R_1 + r_{e4}}} \\ &= \frac{R_{electrode} + r_{e1}}{R_{electrode} + R_1 + r_{e2}} \times \frac{R_{calibration} + R_1 + r_{e4}}{R_{calibration} + r_{e3}} \end{aligned} \tag{5.1}$$

$$V_{ratio} = \frac{p_1 R_{electrode} + p_2}{R_{electrode} + q_1} \tag{5.2}$$

$$R_{electrode} = \frac{p_2 - q_1 V_{ratio}}{V_{ratio} - p_1} \tag{5.3}$$

The Equation 5.2 of best fit was confirmed using `MATLAB` giving $p_1 = 17.4687$, $p_2 = 18.4643$ and $q_1 = 91.8315$ with an r^2 value of 1.0000. The corrected resistance values were then obtained by applying Equation 5.3 to the voltage ratios and these results were graphed and are shown in Figure 5.5 with a gain of 1.0000 and an offset of 0.0000.

Chapter 6

Conclusions

The purpose of this project was to...

This report began with...

The literature review was followed in Chapter...

The bulk of the work for this project followed next, in Chapter...

In Chapter...

Finally, Chapter... attempted to...

In summary, the project achieved the goals that were set out, by designing and demonstrating...

Chapter 7

Recommendations

Bibliography

[1] *The Influence Of Formation Anisotropy Upon Resistivity - Porosity Relationships*, ser. SPWLA Annual Logging Symposium, vol. All Days, 06 1981.

[2] "Mapping salty waters," 2019. [Online]. Available: https://www.esa.int/Applications/Observing_the_Earth/Space_for_our_climate/Mapping_salty_waters

[3] N. Snow and I. D. C. (NSIDC), "Ice sheet quick facts," 2024. [Online]. Available: https://nsidc.org/learn/parts-cryosphere/ice-sheets/ice-sheet-quick-facts

[4] R. H. Stewart, *Introduction to Physical Oceanography*. Texas A&M University Press, 2004. [Online]. Available: https://www.uv.es/hegigui/Kasper/por%20Robert%20H%20Stewart.pdf

[5] R. F. HU Sverdrup, MW Johnson, *The Oceans, Their Physics, Chemistry, and General Biology*. New York: Prentice-Hall, 1942. [Online]. Available: http://ark.cdlib.org/ark:/13030/kt167nb66r/

[6] E. L. Lewis and R. G. Perkin, "Salinity: Its definition and calculation," *Journal of Geophysical Research*, vol. 83, no. C1, pp. 466–478, 1978. [Online]. Available: https://agupubs.onlinelibrary.wiley.com/doi/epdf/10.1029/JC083iC01p00466

[7] Y. Zheng, Y. Liu, J. Zhou, and Y. Wang, "Electrical conductivity of the global ocean," *Earth, Planets and Space*, vol. 69, no. 1, pp. 1–10, 2017.

[8] E. B. editors, "Seawater," *Encyclopædia Britannica*, 2024. [Online]. Available: https://www.britannica.com/science/seawater

[9] W. S. Wooster, A. J. Lee, and G. Dietrich, "Redefinition of salinity," *Journal of Marine Research*, vol. 27, no. 3, 1969.

[10] U. G. Survey, "Water density," 2018. [Online]. Available: https://www.usgs.gov/special-topics/water-science-school/science/water-density#:~:text=A%20common%20unit%20of%20measurement,Celsius%20(39.2Âř%20Fahrenheit).

[11] B. Kjerfve, "Measurement and analysis of water current, temperature, salinity, and density," in *Estuarine hydrography and sedimentation*, K. Dyer, Ed. Cambridge: Cambridge University Press, 1983, pp. 187–226.

[12] U. of Washington Department of Oceanography, "A compilation of articles reporting research," 1966.

[13] H. Schmidt, S. Seitz, E. Hassel, and H. Wolf, "The density–salinity relation of standard seawater," *Ocean Science*, vol. 14, no. 1, pp. 15–40, 2018. [Online]. Available: https://os.copernicus.org/articles/14/15/2018/

[14] C. T. Swift and R. E. Mcintosh, "Considerations for microwave remote sensing of ocean-surface salinity," *IEEE Transactions on Geoscience and Remote Sensing*, vol. GE-21, no. 4, pp. 480–491, 1983.

[15] C. Gabarró, J. Font, A. Camps, M. Vall-llossera, and A. Julià, "A new empirical model of sea surface microwave emissivity for salinity remote sensing," *Geophysical Research Letters*, vol. 31, no. 1, 2004. [Online]. Available: https://agupubs.onlinelibrary.wiley.com/doi/abs/10.1029/2003GL018964

[16] S. Yueh, R. West, W. Wilson, F. Li, E. Njoku, and Y. Rahmat-Samii, "Error sources and feasibility for microwave remote sensing of ocean surface salinity," *IEEE Transactions on Geoscience and Remote Sensing*, vol. 39, no. 5, pp. 1049–1060, 2001.

[17] R. Millard and G. Seaver, "An index of refraction algorithm for seawater over temperature, pressure, salinity, density, and wavelength," *Deep Sea Research Part A. Oceanographic Research Papers*, vol. 37, no. 12, pp. 1909–1926, 1990. [Online]. Available: https://www.sciencedirect.com/science/article/pii/019801499090086B

[18] D. Malardé, Z. Y. Wu, P. Grosso, J.-L. de Bougrenet de la Tocnaye, and M. L. Menn, "High-resolution and compact refractometer for salinity measurements," *Measurement Science and Technology*, vol. 20, no. 1, p. 015204, dec 2008. [Online]. Available: https://dx.doi.org/10.1088/0957-0233/20/1/015204

[19] O. A. Tengesdal, "Measurement of seawater refractive index and salinity by means of optical refraction," Master's thesis, University of Bergen, 2012.

[20] Y. Liao, K. Yang, and X. Shi, "Theoretical study on simultaneous measurement of seawater temperature and salinity based on dual fiber interferometers combined with nonlinear decoupling algorithm," *Measurement*, vol. 211, p. 112596, 2023. [Online]. Available: https://www.sciencedirect.com/science/article/pii/S0263224123001604

[21] S. Yang, J. Xu, L. Ji, Q. Sun, M. Zhang, S. Zhao, and C. Wu, "In situ measurement of deep-sea salinity using optical salinometer based on michelson interferometer," *Journal of Marine Science and Engineering*, vol. 12, no. 9, 2024. [Online]. Available: https://www.mdpi.com/2077-1312/12/9/1569

[22] G. R. C. Possetti, R. C. Kamikawachi, C. L. Prevedello, M. Muller, and J. L. Fabris, "Salinity measurement in water environment with a long period grating based interferometer," *Measurement Science and Technology*, vol. 20, no. 3, p. 034003, feb 2009. [Online]. Available: https://dx.doi.org/10.1088/0957-0233/20/3/034003

[23] L. V. Nguyen, M. Vasiliev, and K. Alameh, "Three-wave fiber fabry–pérot interferometer for simultaneous measurement of temperature and water salinity of seawater," *IEEE Photonics Technology Letters*, vol. 23, no. 7, pp. 450–452, 2011.

[24] Y. Zhao, J. Zhao, Y. Peng, R.-J. Tong, and L. Cai, "Simultaneous measurement of seawater salinity and temperature with composite fiber-optic interferometer," *IEEE Transactions on Instrumentation and Measurement*, vol. 71, pp. 1–8, 2022.

[25] R. Somaraju and J. Trumpf, "Frequency, temperature and salinity variation of the permittivity of seawater," *IEEE Transactions on Antennas and Propagation*, vol. 54, no. 11, pp. 3441–3448, 2006.

[26] O. A. Tengesdal, B. L. Hauge, and L. E. Helseth, "Electromagnetic and optical methods for measurements of salt concentration of water," *Journal of Electromagnetic Analysis and Applications*, vol. 6, no. 6, 2014.

[27] I. O. Commission, "Teos-10: The international thermodynamic equation of seawater (teos-10) for temperature, salinity, density, sound speed, and other oceanographic variables," *Manuals and Guides*, vol. 56, 2010. [Online]. Available: https://www.teos-10.org/pubs/TEOS-10_Manual.pdf

[28] S.-B. Scientific, "Conversion of pressure to depth," 2024. [Online]. Available: https://www.google.com/url?sa=t&rct=j&q=&esrc=s&source=web&cd=&ved=2ahUKEwij6ebU1sCIAxXPiv0HHXDELasQFnoECCMQAQ&url=https%3A%2F%2Fwww.seabird.com%2Fasset-get.download.jsa%3Fid%3D54627861710&usg=AOvVaw1fK2h9jmgpiBuyu8lkM1tl&opi=89978449

[29] T. L. Hill, *An introduction to statistical thermodynamics*. Courier Corporation, 1986.

[30] A. Poisson and M. H. Gadhoumi, "An extension of the practical salinity scale 1978 and the equation of state 1980 to high salinities," *Deep Sea Research Part I: Oceanographic Research Papers*, vol. 40, no. 8, pp. 1689–1698, 1993. [Online]. Available: https://www.sciencedirect.com/science/article/pii/096706379390022U

[31] G. T. Furukawa, J. L. Riddle, and W. R. Bigge, "The international practical temperature scale of 1968 in the region 13.81 k to 90.188 k as maintained at the national bureau of standards," *Journal of Research of the National Bureau of Standards-A. Physics and Chemistry*, vol. 77A, no. 3, pp. 309–322, 1973. [Online]. Available: https://nvlpubs.nist.gov/nistpubs/jres/77A/jresv77An3p309_A1b.pdf

[32] H. Preston-Thomas, "The international temperature scale of 1990 (its-90)," *Metrologia*, vol. 27, no. 107, pp. 3–10, 1990. [Online]. Available: https://www.nist.gov/system/files/documents/pml/div685/grp01/ITS-90_metrologia.pdf

[33] "What is the typical water conductivity range? | atlas scientific," 2022. [Online]. Available: https://www.atlascientific.com/blog/2022/09/water-conductivity-range

[34] F. Walsh, "Electrode reactions in metal finishing," *Transactions of the Institute of Metal Finishing*, vol. 69, pp. 107–111, 08 1991.